

Characterization of the ITER model negative ion source during long pulse operation

R. S. Hemsworth, D. Boilson, B. Crowley, D. Homfray, H. P. L. de Esch, A. Krylov, and L. Svensson

Citation: [Review of Scientific Instruments](#) **77**, 03A511 (2006); doi: 10.1063/1.2164891

View online: <https://doi.org/10.1063/1.2164891>

View Table of Contents: <http://aip.scitation.org/toc/rsi/77/3>

Published by the [American Institute of Physics](#)



Nanopositioning Systems Micropositioning AFM & SPM Single molecule imaging

The image is a promotional banner for Mad City Labs Inc. (MCL). It features a blue background with the company logo at the top center, which consists of the letters 'MCL' in a large, red, stylized font, with 'MAD CITY LABS INC.' written in a smaller, red, sans-serif font below it. Below the logo, there are four distinct images of scientific instruments, each with a corresponding label underneath. From left to right: 1. A large, light-colored, square-shaped nanopositioning system. 2. A smaller, dark-colored, rectangular micropositioning stage. 3. A white and grey AFM & SPM system, with a small inset image showing a striped pattern. 4. A complex, dark-colored single molecule imaging setup, including a main stage and a separate control unit.

Characterization of the ITER model negative ion source during long pulse operation

R. S. Hemsworth^{a)}

Association EURATOM-CEA, CEA Cadarache, F-13108, St. Paul lez Durance, France

D. Boilson

Association EURATOM-DCU, PRL/NCPST, Glasnevin, Dublin 13, Ireland

B. Crowley and D. Homfray

Euratom/UKAEA Fusion Association, Culham Science Centre, Abingdon, OX14 3DB, United Kingdom

H. P. L. de Esch, A. Krylov, and L. Svensson

Association EURATOM-CEA, CEA Cadarache, F-13108, St. Paul lez Durance, France

(Presented on 14 September 2005; published online 21 March 2006)

It is foreseen to operate the neutral beam system of the International Thermonuclear Experimental Reactor (ITER) for pulse lengths extending up to 1 h. The performance of the KAMABOKO III negative ion source, which is a model of the source designed for ITER, is being studied on the MANTIS test bed at Cadarache. This article reports the latest results from the characterization of the ion source, in particular electron energy distribution measurements and the comparison between positive ion and negative ion extraction from the source. © 2006 American Institute of Physics. [DOI: 10.1063/1.2164891]

I. BACKGROUND

The Kamaboko III negative ion source, which was designed and built by JAERI, Naka, Japan, is a model ($\approx 25\%$ in linear dimensions) of the reference design ion source for the International Thermonuclear Experimental Reactor (ITER) neutral beam injectors. The ion source is a magnetic multi-pole, arc discharge, source with 12 tungsten filaments. Cesium is added to the source to enhance the extracted negative ion current density. The source is attached to a three grid accelerator (plasma, extraction and acceleration grids) which can produce beams of ≤ 30 keV. A target located at > 1.2 m from the ion source is used to measure the accelerated current calorimetrically. Although the source has achieved the design parameters during short pulses (< 5 s), during long pulses (> 50 s) the calorimetrically measured negative ion current density is, at the appropriate arc power, $< 60\%$ of that required for ITER.¹ Consequently, a detailed characterization of the source has been undertaken.

II. EXPERIMENTAL RESULTS

We have previously reported the variations in negative ion current, plasma density, plasma electron temperature and fractional dissociation with the arc current and anode to cathode voltage.¹ Here we report on the electron energy distribution and the extraction of negative and positive ions from the ion source.

A. Electron energy distribution measurements

The standard analysis of the Langmuir probe characteristic assumes an isotropic Maxwellian electron energy distribution.

To verify (or show otherwise) that this is the case in the Kamaboko III source, the electron energy distribution (EEDF) 17 mm in front of the plasma grid (PG) has been measured using the Boyd–Twiddy technique² with a 0.9-mm-diam spherical probe. The spherical probe is not sensitive to the isotropy of the electron distribution, unlike cylindrical probes. Figure 1 shows the EEDF measured for an H₂ discharge with an arc power of ≈ 45 kW. There are fewer low energy electrons than would be the case for a Maxwellian EEDF and a clear (but unexplained) peak is seen at ≈ 17.5 eV. A “Laframboise” analysis³ of data from a cylindrical probe, 0.05 mm diameter, 5 mm long, in a similar discharge gave an electron density and “temperature” $\approx 30\%$ lower than these EEDF data.

III. NEGATIVE ION BEAMS

During long pulse operation the current arriving at the target is typically $< 60\%$ of the current taken from the high voltage power supply. The “lost” current is too large to be explained by experimental error. It has been demonstrated that the lost current is not due to accelerated electrons.¹ It is hypothesized that part of the accelerated ion beam is so divergent that $< 60\%$ of the beam is intercepted by the target. A diagnostic drift duct is now installed on MANTIS, see Fig. 2, which is designed to determine if this is correct. Figure 3 shows the geometry of the three grid, 30 keV accelerator used.

The diagnostic duct, which butts against the exit of the accelerator, is 1.2 m long, square in cross section, 0.25×0.25 m², and closed at the end by an uncooled, thermally insulated, 10-mm-thick copper target. The acceleration grid support is ≈ 0.2 m long, so that the source to target distance is ≈ 1.4 m. Each wall of the duct is made of six rectangular copper plates, each 0.2×0.25 m² and 5 mm thick. These

^{a)} Author to whom correspondence should be addressed; electronic mail: ronald.hemsworth@cea.fr

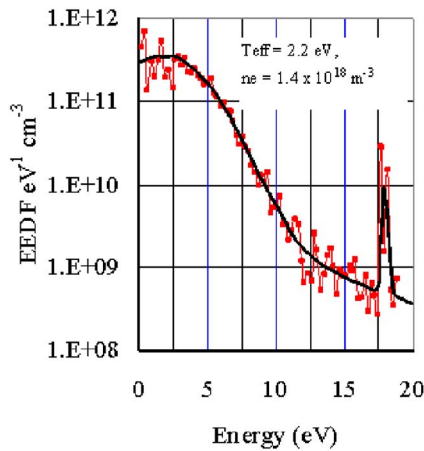


FIG. 1. EEDF measured with a 0.9-mm-diam spherical probe 17 mm in front of the plasma grid; arc power=45 kW, PG floating, 0.3 Pa, H₂.

plates are mounted on, but thermally insulated from, a stainless steel support frame. Two thermocouples are connected to each plate and three to the target. Slots 5 mm wide between each group of panels plus the ≈ 20 mm gaps between the accelerator exit and the duct and the target and the duct allow pumping of the gas leaving the accelerator. Additionally, two copper half cylinders equipped with thermocouples line the walls of the acceleration grid support, from which they are thermally insulated. Calculations have shown that any accelerated electrons are deflected by the long range field of the magnetic filter (located in front of the PG in the ion source) onto the acceleration grid or one of these half cylinders. All the power from the ion beam must fall on the acceleration grid, the duct panels or the target.

It is found that:

- the power accountability, defined as the power to the duct plus that to the target divided by the power taken from the acceleration power supply, is $\approx 90\%$;
- the power to the half cylinders (accelerated electron power exiting the accelerator) is $\approx 1\%$;
- the power to the acceleration grid is $< 5\%$ of the accelerated power; and
- **>30% of the accelerated power falls on the walls of the duct, i.e., there is a very divergent “halo” carrying >30% of the accelerated power. This is not acceptable for the ITER beam source.**

IV. POSITIVE ION BEAMS

In order to establish whether or not the halo is a characteristic of negative ion beams, it was decided to measure the

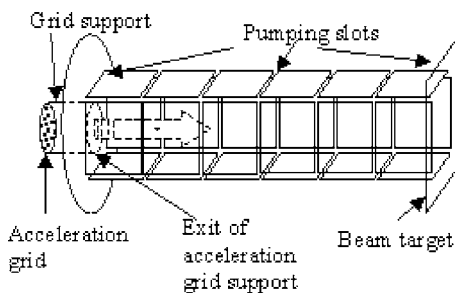


FIG. 2. Schematic of the diagnostic drift duct installed on MANTIS.

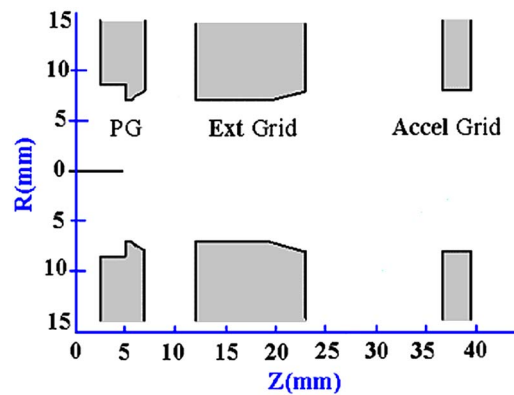


FIG. 3. Schematic of the three grid, 30 keV accelerator. Neither the water cooling nor the electron suppression magnets embedded in the extraction grid are shown.

characteristics of positive ion beams extracted from the same ion source and accelerated by the same accelerator. (For these positive ion studies it was decided not to cesiate the source.)

At the same time as these experiments were started a modern infrared camera became available for these experiments. The camera was set up to view, through a sapphire window, the rear of the beam target (the side not hit by the beam). Some of the target is partly hidden from the IR camera, so the camera is able to give information about the beam optics, but only an estimate of the power incident on the target.

To obtain a measure of the beam divergence the difference between two profiles is obtained, the profile just before the beam pulse and the profile 10 s later. Lateral diffusion during 10 s is significant, therefore simulations which take account of this thermal diffusion have been performed for beams with various values of the beamlet divergence, and these are used to deduce the actual beamlet divergence from the measured profiles.

A problem with accelerating positive ions with this accelerator is that there is no “decel” grid to prevent the extraction of electrons from the plasma created in the drift duct as there is in a conventional positive ion accelerators. It has been shown by calculations that all the electrons extracted from the drift duct would be deflected onto the extraction grid by the magnetic fields in the acceleration gap. Thus the current measured on the extraction grid, I_{G2} , is the sum of the extracted positive ions actually hitting the extraction grid, I_{int}^+ , and the backstreaming electron current, I_e . The power to the extraction grid, P_{G2} is equal to the sum of the power from the positive ions hitting the extraction grid, and the power from the backstreaming electrons, i.e.

$$I_{G2} = I_{int}^+ - I_e, \quad (1)$$

$$P_{G2} = I_{int}^+ * V_{G2} + I_e * (V_{G3} - V_{G2}). \quad (2)$$

As both the current and power to the extraction grid are measured, Eqs. (1) and (2) can be solved to give I_{int}^+ and I_e , and allow the accelerated current, I_{acc} , to be calculated: $I_{acc} = I_{drain} - I_e$, where I_{drain} is the current from the acceleration supply. This analysis assumes that there are no secondary

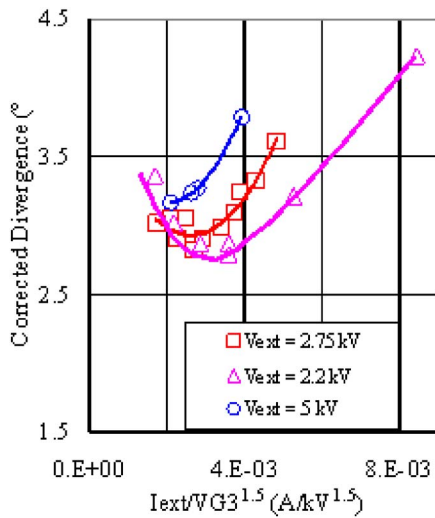


FIG. 4. Beamlet divergence measured in the horizontal direction as a function of the perveance for different values of the extraction voltage. Arc power=20 kW, 0.3 Pa, H₂.

electrons accelerated from the extraction grid to the PG.

It is found that:

- the back streaming electron current is typically 35% of I_{acc} ;
- <5% of the extracted positive ion current hits the extraction grid;
- the total current on the drift duct plus the target derived from the calorimetry is typically >90% of I_{acc} ;
- no power from backstreaming electrons is detected on the rear of the ion source; and
- Up to 90% of the accelerated current falls on the target.

Thus it seems that the 30% halo discussed above is a feature of the negative ion beam.

A. Positive ion beam optics

Figure 4 shows the deduced beamlet divergence as a function of the perveance for different values of the extraction voltage. Figure 5 shows the divergence calculated by SLACCAD⁴ for two of the values of extraction voltage. It can be seen that the measured optimum perveance is in reasonable agreement with the calculated optimum, but the measured divergence is much higher than calculated. This is explained in part because SLACCAD assumes a perfectly uniform ion flux to the plasma grid apertures, and assigns no temperature to the ions.

V. POSITIVE AND NEGATIVE ION EXTRACTION

It has been widely reported that the extracted negative ion current from a negative ion source varies with the extraction voltage.^{5,6} “Normal” positive ion sources, as used for neutral beam injection, show no change in extracted ion current with the extraction voltage. The main difference between these and negative ion sources is that the former have either no magnetic filter or a rather weak filter (<70 G cm), whereas negative ion sources have a strong filter (900 G cm in the Kamaboko III source). Figure 6 shows the positive and

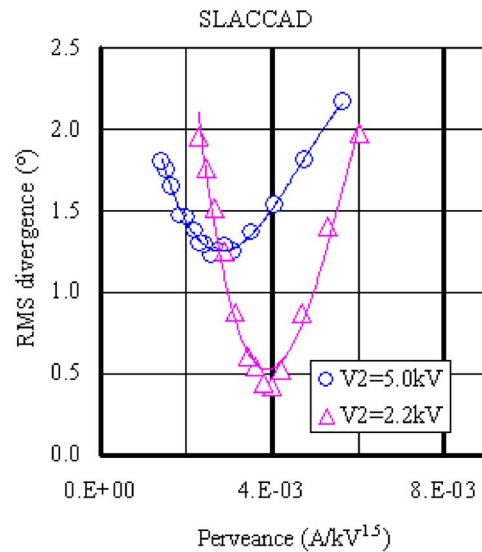


FIG. 5. Beamlet divergence for the Kamaboko III accelerator calculated by SLACCAD.

negative ion current extracted from the Kamaboko III source as a function of the extraction voltage (V_{ext}). Both depend strongly, in an offset quasi-linear fashion, on V_{ext} . Neither exhibit a $V_{ext}^{1.5}$ dependence nor saturation at high values of extraction voltage, as has been found previously.^{5,6}

VI. SUMMARY

The characterization of the Kamaboko III negative ion source has been extended to the measurement of the EEDF 17 mm in front of the plasma grid with a spherical probe, and detailed calorimetry of the accelerated beam. Also a start has been made in comparing positive ion and negative ion extraction from the source using the same extraction system. The EEDF measurements show that the standard type of analysis of Langmuir probe characteristics leads to an underestimation of both the electron density and the electron temperature. The positive ion acceleration shows that the SLACCAD code correctly predicts the optimum perveance, but

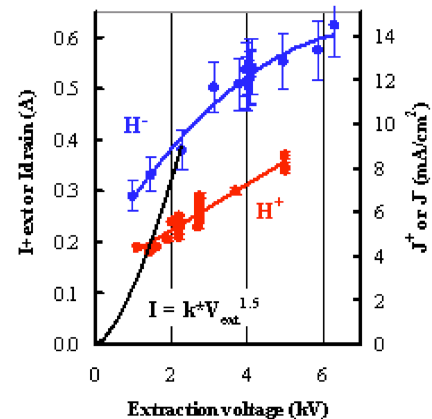


FIG. 6. Positive and negative ion currents (I_{ext}^+ and I_{drain}) and current densities (J^+ and J^-) extracted from the Kamaboko III source vs the extraction voltage. The negative ion data have been corrected for drift (in time) due to tungsten contamination of the plasma grid surface. The H⁺ data were taken with an arc power of 45 kW, the H⁻ data with 20 kW, both with 0.3 Pa, H₂.

underestimates substantially the beamlet divergence. The beam calorimetry reveals a large halo in the accelerated negative ion beams, which carries $\approx 35\%$ of the accelerated beam power. Such a halo is not found with positive ion beams, where $>90\%$ of the accelerated beam impinges on the target. Unlike conventional positive ion sources, the extracted positive ion current varies with the applied extraction voltage, as does the extracted negative ion current. This is most likely due to the strong magnetic filter in the ion source.

- ¹R. S. Hemsworth *et al.*, Proceedings of the 10th International Symposium on the Prod. and Neutralization of Negative Ions and Beams, Kiev, Ukraine, [AIP Conf. Proc., **763**, 3 2004].
- ²R. L. F. Boyd and N. D. Twiddy, Proc. R. Soc. London, Ser. A, **250**, 53 (1959).
- ³J. G. Laframboise, University of Toronto, Institute Aerospace Studies Report No. 100, 1966.
- ⁴J. Paméla, Rev. Sci. Instrum. **62**, 1163 (1991).
- ⁵M. Hanada *et al.*, Proceedings of the 17th IAEA Fusion Energy Conference, Yokohama, Japan, 1999 (unpublished).
- ⁶R. Trainham *et al.*, Rev. Sci. Instrum. **69**, 926 (1998).